Fundus image registration for vestibularis research

Vamsi K. Ithapu[a], Armin Fritsche[b], Ariane Oppelt[c], Martin Westhofen[c], and Thomas M. Deserno[b]

[a]Dept. of Electrical & Computer Engineering, IIT Guwahati, India
[b]Dept. of Medical Informatics, RWTH Aachen University, Aachen, Germany
[c]Dept. of Otorhinolaryngology & Plastic Surgery, RWTH Aachen University, Aachen, Germany

ABSTRACT

In research on vestibular nerve disorders, fundus images of both left and right eyes are acquired systematically to precisely assess the rotation of the eye ball that is induced by the rotation of entire head. The measurement is still carried out manually. Although various methods have been proposed for medical image registration, robust detection of rotation especially in images with varied quality in terms of illumination, aberrations, blur and noise still is challenging. This paper evaluates registration algorithms operating on different levels of semantics: (*i*) data-based using Fourier transform and log polar maps; (*ii*) point-based using scaled image feature transform (SIFT); (*iii*) edge-based using Canny edge maps; (*iv*) object-based using matched filters for vessel detection; (*v*) scene-based detecting papilla and macula automatically and (*vi*) manually by two independent medical experts. For evaluation, a database of 22 patients is used, where each of left and right eye images is captured in upright head position and in lateral tilt of $\pm 20^0$. For 66 pairs of images (132 in total), the results are compared with ground truth, and the performance measures are tabulated. Best correctness of 89.3% were obtained using the pixel-based method and allowing 2.5° deviation from the manual measures. However, the evaluation shows that for applications in computer-aided diagnosis involving a large set of images with varied quality, like in vestibularis research, registration methods based on a single level of semantics are not sufficiently robust. A multi-level semantics approach will improve the results since failure occur on different images.

Keywords: Fundus image, registration, ground truth, semantics

1. INTRODUCTION

Vestibular function in man is organized by the vestibular system to maintain orientation of state and visual perception. The visual cue and the visual contribution for the reflex movements of the eye during head/eye-coordination are performed by visual sensory input to the vestibular central nervous system (CNS). The signal processing in the CNS is used for the regulation of retinal image stability during head movements. Image stability during lateral tilt of the head, which belongs to the natural head and body movement, is performed by means of ocular counter rolling, which is part of the vestibulo-ocular reflex.[1] The position of the retinal image is controlled due to the gravitoinertial force. This force is sensed as a linear acceleration by the gravitational sensory organs of the labyrinth, the otolith organs. The otholith vestibulo-ocular reflex (oVOR) stabilizes the retinal image in a position parallel to the gravitoinertial force. Therefore lateral head tilt results in ocular counter rolling.

In normals the maximum deviation of the binocular eye position is approximately $\pm 4°$.[2] In case of unilateral vestibular deficits as seen in vestibular neuritis or temporal bone fractures cyclorotation of the eye, more than 12° in the ipsilateral direction is observed. Therefore, the so called ocular tilt reaction is described in case of unilateral vestibular function loss during the early phase of the lesion.[3] Measurement of the eye position in case of lateral tilt of the head can be done with use of non-mydriatic fundus photography. The evaluation of the examination consists of the comparison between retinal images in upright head position and in lateral head tilt

Send correspondence to:
Prof. Dr. Thomas M. Deserno
Dept. of Medical Informatics, RWTH Aachen University, 52057 Aachen, Germany
E-mail: deserno@ieee.org, Telephone: +49 241 80 88793, Fax: +49 241 80 33 88793

Medical Imaging 2010: Computer-Aided Diagnosis, edited by Nico Karssemeijer, Ronald M. Summers,
Proc. of SPIE Vol. 7624, 76243E · © 2010 SPIE · CCC code: 1605-7422/10/$18 · doi: 10.1117/12.844475

of 20°. The reliability of the findings depends on the accuracy of position measurement of the retinal images before and after the head tilting procedure. Up to now, the retinal image comparison is based on the deviation of the axis between fovea and papilla, which is analyzed manually. As the contours of those two structures are not well defined, more than 15% variance in measurement disturb the clinical routine application. Therefore, the position of the retinal vascular image should be defined, and the rotation of the vascular pattern during cyclotorsion of the eye has to be evaluated.

This rotation of the vascular pattern is determined by registering the reference image with respect to the rotation induced ones. In general, an image always provides information in various levels of semantics i.e. it is coded symbolically by specific objects or iconically with all pixels in the image. Registration methods extract different types of information content form these semantics. Based on this semantics and the type of information extracted, registration is classified into five groups:

1. *data-based*, relying on the entire image,[4,5]
2. *pixel-based*, using point matching techniques on various gray,[6,7]
3. *edge-based*, trying to extract and compare the edges,[8,9]
4. *object-based*, detecting distinct objects in the image and using their inherent landmarks,[10–12] and
5. *scene-based*, comparing the constellation of certain objects in the images.

The task of registration in vestibularis research is to precisely determine the rotation parameter associated with the eye ball, which is induced by the rotation of entire head. Various methods have been proposed in this regard,[8,13,14] but each algorithm has its own limitations in performance because of the noise arising mainly from non-uniform illumination, aberrations due to optical systems, and blur. However, all these methods can again be differentiated into above mentioned five categories.

The remainder of this paper is organized as follows: Section 2 describes the mathematical background of five different registration methods that are based on the semantics discussed above. In Section 3, the ground truth for evaluation is established. Section 4 shows the results and proposes the multi-semantic level registration and section 5 concludes the paper.

2. MATERIAL AND METHODS

2.1 Image Database

Fundus images of patients suffering from different neural disorders as well as from healthy subjects were collected at University Hospotal of aachen University, Aachen, Germany. For each patient, six images of both left and right eye are taken in upright head position and in lateral head tilt of $\pm 20°$. The images were captured using a non-mydriatic fundus camera (NM-1000, Nidek Corporation, Albignasego, Italy) and stored digitally with a resolution of $1,280 \times 960$ pixels using lossless compression. A database of 132 images is formed from 22 patients representing a great variety of image quality (Fig. 1).

Since only the amount of rotation is clinically important, the image quality may be much lower than in databases such as Digital Retinal Images for Vessel Extraction (DRIVE*), where vessels need to be detected.

2.2 Ground Truth

To establish a ground truth, a medical expert marked the center points of the papilla (also referred to as optic disc) and macula (also referred to as blind spot) manually. To assess inter-operator variability, a second manual reference labeling was independently performed by another physician. In the manual procedure, the centers of macula and papilla are used to calculate the angulation differences.

2.3 Registration Methods

As discussed above five different methods based on the five levels of semantics are investigated. In this section, mathematical and algorithmic detail of each method is addressed. First the intuitive idea is presented followed by analysis specific to the type of information in a fundus image.

*http://www.isi.uu.nl/Research/Databases/DRIVE

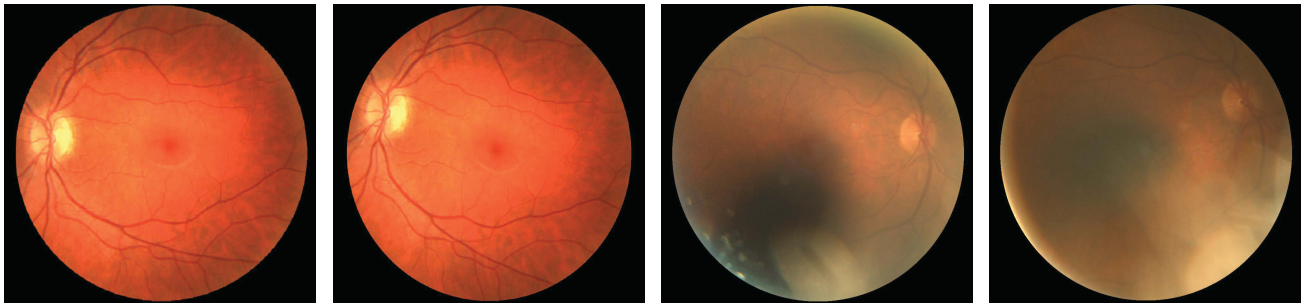

(a) (b) (c) (d)

Figure 1: Variety of images in database. (a, b): set with good quality; (c, d) set with poor quality.

2.3.1 Data Level

As its name suggests, the algorithms at this level use the entire data available i.e., the entire image for registration. Consider two images $f_1(x, y)$ and $f_2(x, y)$ where $f_2(x, y)$ is a translated, rotated and scaled replica of $f_1(x, y)$:

$$f_2(x, y) = f_1[\sigma^{-1}(x\cos\theta_0 + y\sin\theta_0) - x_0, \sigma^{-1}(y\cos\theta_0 - x\sin\theta_0) - y_0] \tag{1}$$

To register these images, the rotation and scaling compensation is done before translation is compensated. Neglecting x_0 and y_0 in the first step, the polar representation $f_{1\rho}(\rho, \theta)$ and $f_{2\rho}(\rho, \theta)$ are related by

$$f_{2\rho}(\rho, \theta) = f_{1\rho}(\rho/\sigma, \theta - \theta_0) \tag{2}$$

Converting (2) to logarithmic axis yields[8]

$$f_{2l\rho}(\lambda, \theta) = f_{1l\rho}(\lambda - \lambda_0, \theta - \theta_0) \tag{3}$$

where $\lambda_0 = \log\sigma$. Hence using the log polar transform, we have converted the rotational and scaling parameters σ and θ_0 into translational movement. Taking the Fourier transform, we get

$$F_{2l}(\epsilon, \eta) = F_{1l}(\epsilon, \eta) * e^{-j2\pi(\epsilon\lambda_0 - \eta\theta_0)} \tag{4}$$

The cross power spectrum of F_{1l} and F_{2l} is $e^{j2\pi(\epsilon\lambda_0 + \eta\theta_0)}$. Note that translational movements in the spatial domain are purely represented on the imaginary axis in the frequency domain, and hence to not affect the magnitude of the Fourier transform. Therefore, neglecting X_0 and y_0 is justified.

Taking the inverse fast Fourier transform (IFFT), we get an approximate impulse function of the form $\delta(\lambda+\lambda_0, \theta+\theta_0)$ in the (λ, θ) domain. In this way, rotation and scaling parameters are detected. The translational parameters x_0 and y_0 are then determined using similar technique on the re-rotated and re-scaled image.[8] Algorithm 1 summarizes the steps involved in this data level registration algorithm.

Algorithm 1: Data level	
1.	Apply log polar transform to each input image
2.	Generate cross power spectrum of the log polar maps
3.	Determine rotation and scaling parameters from maximum
4.	Re-rotate and re-scale reference image
5.	Determine translation parameters by using the output of Step 4 and repeating Steps 2 and 3

If there is no output, the images are rejected. Also note that the rotation parameter is what we are interested in here, which is obtained in Step 3 of the algorithm itself. For evaluation purpose and comparing the performance with other registration algorithms, complete algorithm is implemented on all image pairs.

Consider the color fundus images in Fig. 1a, 1b. The above discussed log polar transform is used to convert the scale and rotation parameters between the images into translation parameters (Fig. 2a, 2b). The cross power

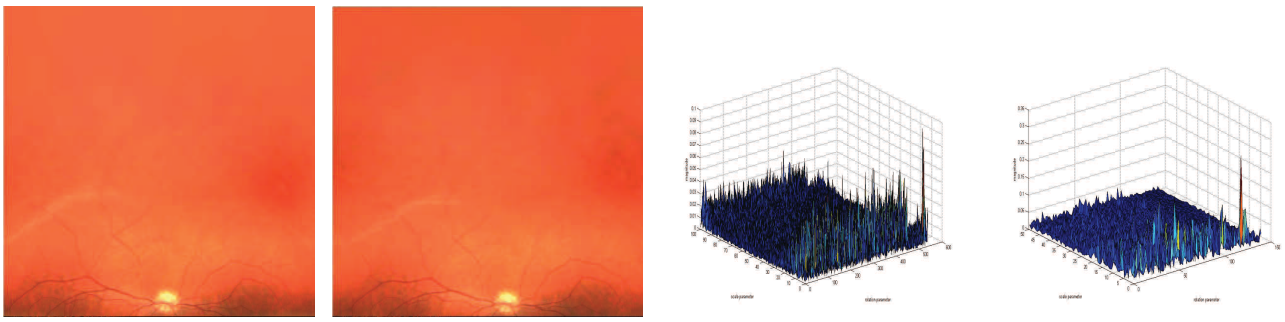

(a) (b) (c) (d)

Figure 2: Data-based method. The log polar image of Fig. 1a and Fig. 1a are displayed in (a) and (b), respectively. Panel (c) shows the cross power spectrum of (a) and (b), while (d) zooms the maximum magnitude of (c) at the point of matching.

spectrum of the Fourier transform of these log polar maps is shown in Fig. 2c, which is then analyzed to determine the rotation and scaling (Fig. 2d). Translation is then determined using similar technique on the re-scaled and re-rotated images.

2.3.2 Pixel Level

On the pixel level, interesting points (IPs) are extracted and compared. The registration of the fundus images is calculated from the best matching of the feature points. Currently, the scale invariant feature transform (SIFT) is the most common algorithm for feature point extraction.[15] It is based on local extremes at the difference of Gaussian (DOG). The descriptors of the IPs are patches of Gaussian-weighted gradients around these points. This allows an easy comparison of two points by using the Euclidean distance between the two feature vectors.

For registration, IPs of two images are extracted. The matching is computed by a simple nearest neighbor (NN) method, associated with the Euclidean distance of the descriptors. To discard the bad matches of feature points, a threshold is defined. Since a global threshold does not perform well, we require the ratio between the closest and second-closest NN to exceed 0.8.[15] If less than three matches of feature points are found, the two images are rejected, since no affine registration is possible.

In order to discard incurred matching in the boundary region of the fundus images, a random samples consensus (RANSAC) algorithm[16] is performed. An affine registration with each subset of three point-matchings is done. All matches, which do not agree with this registration are discarded. Finally the registration, with the least number of discarded matching is chosen. Algorithm 2 summarizes the final registration algorithm operating on the pixel level.

Algorithm 2: Data level	
1.	Extract IPs from each image using the SIFT algorithm
2.	Match the two point clouds by nearest neighbor
3.	Apply the RANSAC algorithm
4.	Discard unmatched correspondences
5.	Re-rotate reference image
6.	Apply affine transform for scaling and translation

For the example image in Fig.1a, feature points are extracted (Fig.3a). Two point clouds are matched using a nearest neighbor method in the SIFT feature space as in Fig.3b, and the final output of RANSAC algorithm looks as in Fig.3c. Later these points are used for an affine registration.

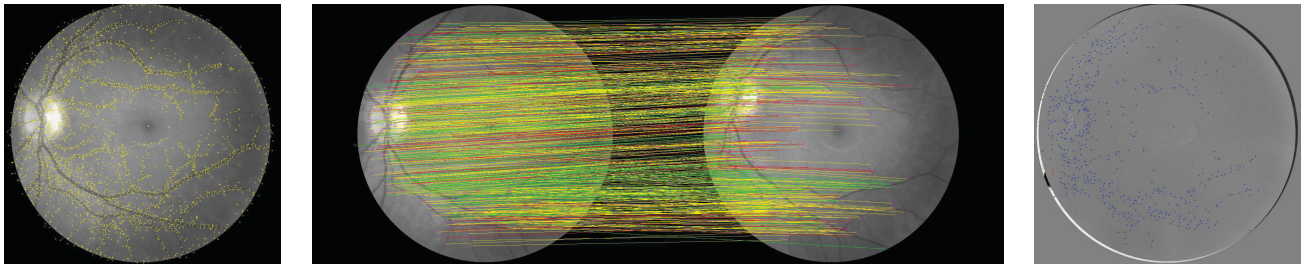

(a) (b) (c)

Figure 3: Pixel-based method. (a): SIFT points in Fig. 1a; (b): nearest neighbor point cloud matching between the SIFT-Points (red lines: Euclidean distance > 0.2, yellow lines: $0.2 \geq$ Euclidean distance > 0.1, green lines: Euclidean distance ≤ 0.1); (c): difference image with accepted correspondences (blue crosses) and discarded correspondences (red lines between two red crosses).

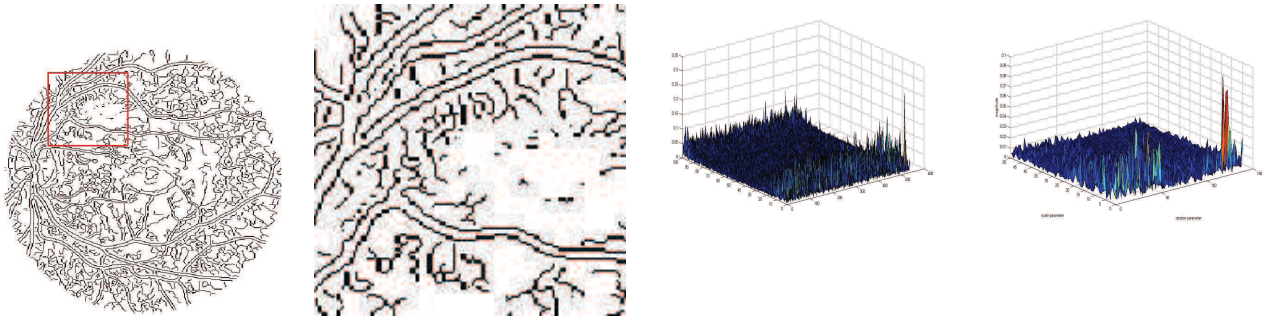

(a) (b) (c) (d)

Figure 4: Edge-based method. (a): Canny edge map of Fig. 1a; (b): edges detected in the red marked square region of (a); (c): cross power spectrum log polar edge maps; (d): maximum magnitude of (c) at the point of matching.

2.3.3 Edge Level

Consider the fundus images represented in the red-green-blue (RGB) color model. The red channel preserves most of the information in the dark regions, i.e., macula and vessels. On the other hand, blue and green channels have almost even illumination throughout the image. Hence edge extraction is performed in the red channel. The various steps involved in this edge level registration procedure are summarized in Algorithm 3.[8]

Algorithm 3: Edge level	
1.	Extract the red channel of each input image
2.	Generate Canny edge maps
3.	Morphologically dilate resulting Canny maps using a 9×9 mask
4.	Apply log polar transform on dilated Canny maps
5.	Generate cross power spectrum of the log polar maps
6.	Determine rotation and scaling parameters
7.	Re-rotate and re-scale reference image
8.	Use the output of step 6 and repeat step 2 and 3 to determine the translation parameter

If Step 8 gives no reliable output, the images are rejected. Again testing this algorithm using the images in Fig. 1a, 1b, we get the dilated canny maps as in Fig. 4a, 4b. These maps then are processed for registration as outlined above (Fig. 4c, 4d).

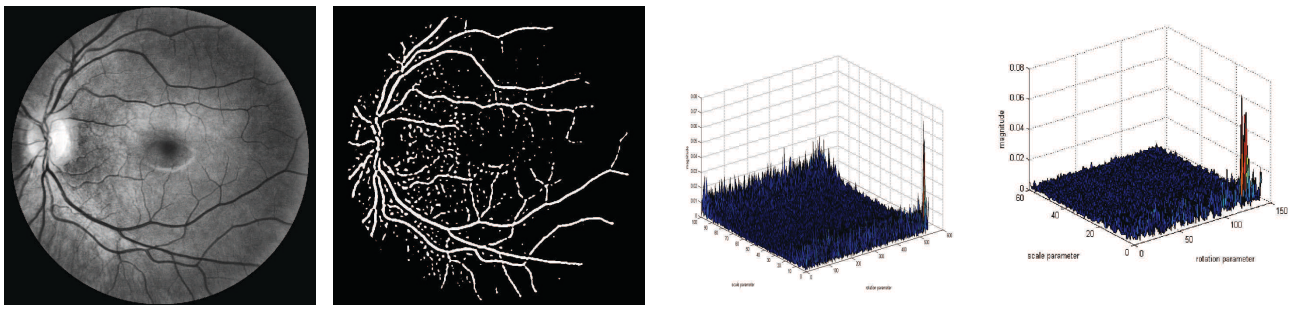

(a) (b) (c) (d)

Figure 5: Object-based method. (a): adaptive histogram equalization of red channel of Fig. 1a, enhancing vessel information; (b): matched filter detection of vessels; (c): cross power spectrum log polar vessel maps; (d): maximum magnitude of (c) at the point of matching.

2.3.4 Object Level

Registration operating on the object level of semantics uses specific information obtained from well-defined objects, which are common to all the images under consideration. In fundus imaging, such objects are the macula, the papilla and the vessels. The brightness level, area covered and orientation of these objects varies for each image, and help in registering two images if one can precisely extract this information.

Here, we deal with information from only one of such dominant objects, i.e., the vessels. In fundus images, vessels can be modeled by a certain gray scale function, basically the contrast between vessels and retina – and within the vessels, from wall to wall. This is modeled with matched filters. Using this idea, the entire vessel tree is detected. Again, red channel is chosen for the process and to enhance the information content in the form of vessels, which are mostly concentrated in dark regions, adaptive histogram equalization is applied. The noise in this equalized channel is filtered out and, finally, passed through a matched filter that detects vessels using template matching algorithm.[17] The complete procedure followed for registration follows Algorithm 4.

Algorithm 4: Object level	
1.	Extract the red channel for both images
2.	Apply adaptive histogram equalization
3.	Remove noise applying a Gaussian band pass filter (center frequency 0.06, variance 0.0004)
4.	Create 12 matched filter (width 8, orientation from 0° to 165°, step 15°)
5.	Collect maximum responses from filtering output of Step 3 with templates of Step 4
6.	Apply log polar transform to obtained vessel trees
7.	Generate cross power spectrum of log polar maps
8.	Determine rotation and scaling parameters
9.	Re-rotate and re-scale reference image
10.	Determine the translation parameter repeating Steps 7 and 8 to output of Step 9

If the final registered parameters are not reliable, the images are rejected from registration. The effect of this algorithm is visualized in Figure 5. Fig. 5a represents the histogram-equalized version of the original image (Fig. 1a). Fig. 5b shows the vessel map after template matching, and Figs. 5c, 5d show the cross power spectrum, which is used for estimating the rotation parameter.

2.3.5 Scene Level

The last level of semantics deals with scenes in the images. On scene level of image understanding, several objects are regarded in their particular constellation. similar to manual registration, our approach is based on papilla and macula, where the center of gravity of both is used to construct the geometric dependencies and compute the rotation angle. In other words, this scene alignment of papilla-macula can be used for registering two different fundus images of the same person.

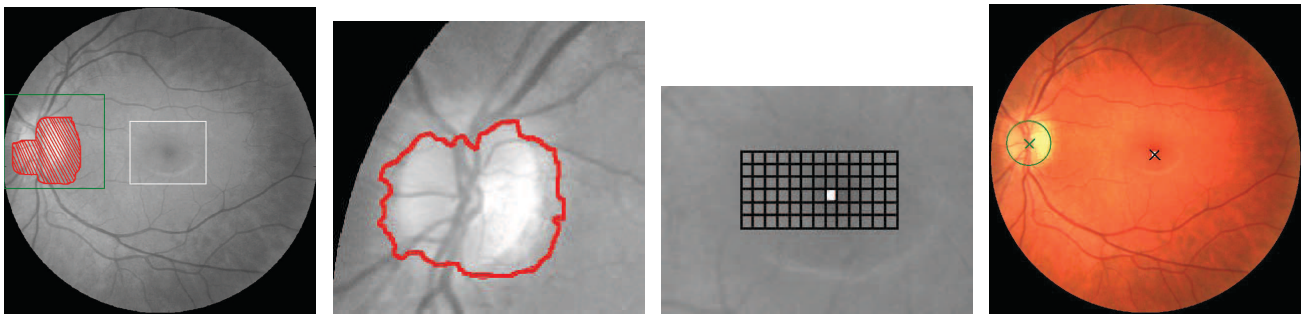

(a) (b) (c) (d)

Figure 6: Scene-based method. (a): mean segmentation clustering output of Fig. 1a with highest index cluster shaded by red lines; (b): level set active contour detection in green square region of (a), red boundary is the final level set function; (c): detecting the macula, white shaded grid is the best candidate for macula center; (d): final coordinated used for geometric reconstruction.

Again, the algorithm is based on the red channel. The papilla appears bright whereas the macula, which is positioned at the center of the fundus image, appears rather dark. Hence, we segment the region with highest gray scale index.[18] The optic disc is present inside this region, which is then used as a initial contour to a level set active contour detection algorithm.[19] At each step of this algorithm, the area of the contour is calculated and used to control the iteration. If the iteration ends before reaching the threshold point, a circular disc template (area = 8100 pixels) matching is done to select the best fitting disc as papilla. Else, the determined contour is used to predict the expected papilla region. Finally, the center of mass of the automatically detected papilla is used as landmark. Furthermore, the macula is modeled as the darkest region at the center of the image. To determine its center of mass, a region of interest (100×100 pixel) is extracted from the image center and subdivided into squared grids (4×4 pixel). The grid with least mass (darkest pixels) is selected as center of macula. The step by step procedure following these guidelines is summarized in Algorithm 5.

Algorithm 5: Scene level	
1.	Extract the red channel of the images
2.	Apply mean-shift segmentation with spatial domain bandwidth of 10 and range domain bandwidth of 7.5
3.	Select the cluster with highest index
4.	Extract the boundary of the cluster
5.	Apply level set active contour detection algorithm; call the output "processed contour"
6.	If (area of processed contour $\geq$ 8100 pixels) or (processed contour $\neq$ current contour) assign current contour = processed contour and goto step 5. Else goto step 7
7.	If (area of processed contour $<$ 8100 pixels) goto step 9
8.	Apply circular disc template (area = 8100 pixels) on the given contour region and detect the best fitting disc
9.	Calculate the center of mass of the final disc region, which is the estimated center of papilla
10.	Select a 100×100 template region at the center of the red channel
11.	Divide the selected region of step 10 into 625 4×4 grids
12.	Determine the grid with least mass; call it the estimated macula
13.	After applying step 1 to 12 for both images, calculate the rotation parameter using basic trigonometry

The final output of Algorithm 5 is the estimated rotation parameter for each image pair under consideration. If the mean-shift segmentation fails, the images are rejected from registration. Algorithm 5 is visualized in Figure 6. For the image in Fig. 1a, the output of Step 2 is shown in Fig. 6a. The boundary of the initial cluster is visualized in Fig. 6b and the grid used for macula detection is shown in Fig. 6c. Finally, the center of papilla and macula are marked in Fig. 6d.

Table 1: Evaluation of the five registration methods and manual recording

Registration method	Average run-time	Rejection rate (in %)	$\|\Delta\| < 0.5^0$		$\|\Delta\| < 1.5^0$		$\|\Delta\| < 2.5^0$	
			correct	wrong	correct	wrong	correct	wrong
Data-based	2 sec	19.7	42.4	37.9	48.4	31.9	72.7	7.6
Pixel-based	∼min	9.1	62.1	28.8	**71.2**	19.7	**89.3**	1.6
Edge-based	2.2 sec	18.1	43.9	38	62.2	19.7	78.7	3.2
Object-based	13.5 sec	**7.5**	**63.8**	28.7	69.7	22.7	87.8	4.6
Scene-based	∼min	10.6	57.5	31.9	66.7	22.7	84.8	4.6
Manual	∼sec	0	94.0	6.0	95.4	4.6	95.4	4.6

3. EVALUATION

Based on the compiled image database, registration is done with each algorithm. Although the manually established ground truth may be erroneous, we compute the deviation Δ of the rotation determined by the algorithms and the manually performed ground truth. The second manual reference labeling is regarded as sixth algorithm. The number of rejected image pairs is protocoled. Subtraction images are calculated to visualize the structured noise[20] that is remaining in the iomages. Also, MatLab execution times were recorded.

4. RESULTS

Allowing mis-angulations of 0.5° from the manual ground truth, the object-based method using vessel information is slightly superior (correctness rate 63.8%) to the pixel-based method (62.1%), which turns out best for $|\Delta| < 1.5°$ and $|\Delta| < 2.5°$, where it reaches correctness rates of 71.2% and 89.3%, respectively (Table 1). The manual registration performed with 95% of all of the cases. Data-, edge-, and object-based techniques are computed within seconds, while the other may need several minutes depending on the input images. Subtraction images are exemplified in Fig. 7.

5. DISCUSSION

Not surprisingly, the medical experts' ground truth turned out to be unreliable. As it can be seen in Fig. 7, the automatic pixel-based method may be superior to the ground truth. Success rates of manual methods are 95% showing the inter-operator variability. Combining the techniques with lowest rejection rates, i.e., pixel-based and object-based (vessels), the rejection rate decries to 4.3%, since only three of the seven pairs that have been rejected in the pixel-based method are identical to the rejections of the object-based approach. In our example, the scene-based method additionally reduces the number of rejections (3.2% remaining), Hence, applying a multi-level semantics approach for further evaluation may reach the required robustness for clinical applications. In future, this will be comprehensively evaluated, also using a larger data set.

In conclusion, it has been shown, that registration methods operating on different levels of semantics perform differently in the given application. However, a higher level of semantics does not guarantee better performance. Contrarily, the pixel-based method based on SIFT features performed best. However, any method based on only a single level of semantics is shown to be not suitable to develop sufficiently robust algorithms as required for fundus images that have not been acquired for vessel detection. Rejection rates of 10% are too high. Combining two or more levels of semantics, more information about the characteristics of the image signal can be extracted and the number of instances where registration fails can be reduced considerably, as failure occurs on different images. This finding may apply to all medical images which are generally characterized by non uniform illumination, high noise content due to aberrations and blur.

REFERENCES

[1] Diamond S, Markham C, Furuya N. Binocular counterrolling during sustained body tilt in normal humans and in a patient with unilateral vestibular nerve section. Ann Otol Rhinol Laryngol. 1982;91(1):225–9.

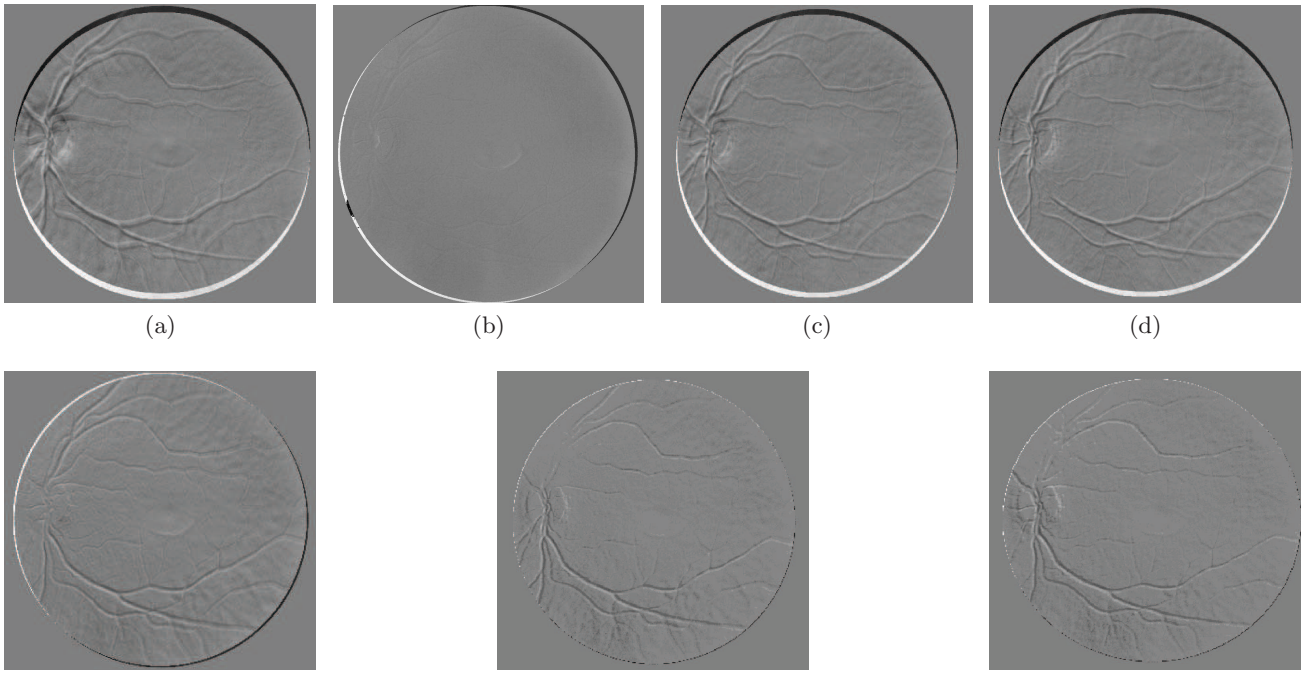

(a) (b) (c) (d)

(e) (f) (g)

Figure 7: Subtraction images. (a): data-based; (b): pixel-based; (c): edge-based; (d): object-based; (e): scene-based; (f): manual measurement, (g): ground truth.

[2] Brandt T, Dieterich M. Cyclorotation of the the eyes and subjective visual vertical in vestibular brain stem lesions. Ann N Y Acad Sci. 1992;656:537–49.

[3] Halmagyi G, Gresty G, Gibson W. Ocular tilt reaction with peripheral vestibular lesion. Ann Neurol. 1979;6(1):80–3.

[4] Reddy BS, Chattarjee BN. An FFT-based technique for translation, rotation, and scale-invariant image registration. IEEE Trans Image Process. 1996;5(8):1266–71.

[5] Wolberg G, Zokai S. Robust image registration using log-polar transform. Proc ICIP. 2000;p. 493–6.

[6] Moradi M, Abolmaesumi P. Medical image registration based on distinctive image features from scale-invariant (SIFT) keypoints. Int Congr Ser. 2005;1281:1292.

[7] Moradi M, Abolmaesumi P. Deformable registration using scale-space keypoints. Proc Soc Photo Opt Instrum Eng. 2006;6144:791–8.

[8] Wang W, Chen H, Li J, Yu J. A Registration method of fundus images based on edge detection and phase-correlation. Proc ICICIC. 2006;p. 572–6.

[9] JunWei H. Image registration using a new edge-based approach. Comput Vis Image Underst. 1997;67(2):112–30.

[10] Turgay C, Kai-Kuang M. Fast object-based image registration using principal component analysis for super-resolution imaging. Proc VIE. 2008;p. 705–10.

[11] Rohrer J, Gong L. Focused atlas-based image registration for recognition. Proc ICIP. 2008;p. 1808–11.

[12] Chaudhuri S, Chatterjee S. Detection of blood vessels in retinal images using two-dimensional matched filters. IEEE Trans Med Imaging. 1989;8(3):263–9.

[13] Laliberte F, Gagnon L, Sheng Y. Registration and fusion of retinal images-an evaluation study. IEEE Trans Med Imaging. 2003;22(5):661–73.

[14] Matsopoulos G, Mouravliansky N. Automatic retinal image registration scheme using global optimization techniques. IEEE Trans Inf Technol Biomed. 1999;3(1):47–60.

[15] Lowe D. Distinctive image features from scale-invariant key points. Int J Computer Vis. 2004;60(2):91–110.

[16] Fischler M, Bolles R. Random sample consensus: A paradigm for model fitting with applications to image analysis and automated cartography. Commun ACM. 1981;24(6):381–95.
[17] Youssif A, Ghalwash A. Detection of blood vessels in retinal images using two-dimensional matched filters. IEEE Trans Med Imaging. 2008;27(1):11–9.
[18] Guo H, Guo P, Lu H. A fast mean shift procedure with new iteration strategy and re-sampling. Proc IEEE SMC. 2006;p. 2385–9.
[19] Xu J, Chutatape O, Chew P. Optic disk boundary detection by modified active contour model. IEEE Trans Biomed Eng. 2007;54(6):473–82.
[20] Lehmann T, Sovakar A. A comparision of mathematical similarity measures for digital subtraction radiography. Comput Biol Med. 1997;27:151–67.